Effect of chlorpyrifos on freshwater microbial community and metabolic capacity of zebrafish

Xu, N.; Zhou, Z.; Chen, B.; Zhang, Z.; Zhang, J.; Li, Y.; ... ; Qian, H.

Ecotoxicology and Environmental Safety 262 (2023) 115230

Contents lists available at ScienceDirect

Ecotoxicology and Environmental Safety

journal homepage: www.elsevier.com/locate/ecoenv

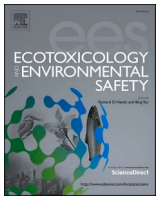

Effect of chlorpyrifos on freshwater microbial community and metabolic capacity of zebrafish

Nuohan Xu [a], Zhigao Zhou [a,b], Bingfeng Chen [a], Zhenyan Zhang [a], Jinfeng Zhang [a], Yan Li [a], Tao Lu [a], Liwei Sun [a], W.J.G.M. Peijnenburg [c,d], Haifeng Qian [a,*]

[a] College of Environment, Zhejiang University of Technology, Hangzhou 310032, PR China
[b] Zhejiang Province Institute of Architectural Design and Research, Hangzhou 310000, PR China
[c] Institute of Environmental Sciences (CML), Leiden University, RA Leiden 2300, the Netherlands
[d] National Institute of Public Health and the Environment (RIVM), Center for Safety of Substances and Products, P.O. Box 1, Bilthoven, the Netherlands

ARTICLE INFO

Edited by Bing Yan

Keywords:
Chlorpyrifos
Aquatic toxicity
Microbial community
Antibiotic resistance genes
Zebrafish

ABSTRACT

Chlorpyrifos is a widely used organophosphorus insecticide because of its high efficiency and overall effectiveness, and it is commonly detected in aquatic ecosystems. However, at present, the impact of chlorpyrifos on the aquatic micro-ecological environment is still poorly understood. Here, we established aquatic microcosm systems treated with 0.2 and 2.0 μg/L chlorpyrifos, and employed omics biotechnology, including metagenomics and 16S rRNA gene sequencing, to investigate the effect of chlorpyrifos on the composition and functional potential of the aquatic and zebrafish intestinal microbiomes after 7 d and 14 d chlorpyrifos treatment. After 14 d chlorpyrifos treatment, the aquatic microbial community was adversely affected in terms of its composition, structure, and stability, while its diversity showed only a slight impact. Most functions, especially capacities for environmental information processing and metabolism, were destroyed by chlorpyrifos treatment for 14 d. We observed that chlorpyrifos increased the number of risky antibiotic resistance genes and aggravated the growth of human pathogens. Although no clear effects on the structure of the zebrafish intestinal microbial community were observed, chlorpyrifos treatment did alter the metabolic capacity of the zebrafish. Our study highlights the ecological risk of chlorpyrifos to the aquatic environment and provides a theoretical basis for the rational use of pesticides in agricultural production.

1. Introduction

Conflicts among food, population, and environment are increasingly evident globally. Humans require increased agricultural productivity to feed a growing global population (Rohr et al., 2019), and efforts to control the spread of vector-borne diseases must intensify under the pressure of global climate change (Caminade et al., 2019). This has consequently increased the human dependence on pesticides. Approximately 3.5 million tons of pesticides are used yearly to enhance productivity and inhibit insects, weeds, and pathogens (Sharma et al., 2019). Chlorpyrifos is an organophosphorus insecticide in agriculture to control a variety of pests, including insects, rodents, fungi, and other plant pathogens, because of its high efficiency and broad effectiveness (Huang et al., 2021; Malakootian et al., 2020). Chlorpyrifos has thus become the most used organophosphorus insecticide globally today (Echeverri-Jaramillo et al., 2021). Global chlorpyrifos usage in 2015 exceeded 200,000 tons and was expected to continue growing (John and Shaike, 2015). Extensive chlorpyrifos used in soil leads to aquatic pollution through rainwater and surface runoff (Sumon et al., 2018). Residual chlorpyrifos concentrations in a Bangladesh lake ranged from 3.27 to 9.31 μg/L (Hossain et al., 2015), and a concentration of 70.5 ng/L chlorpyrifos was detected in Californian river surface water (Starner et al., 2005). All of these concentrations exceed environmental standards in the aquatic environment. Consequently, quantifying and assessing the environmental effects of chlorpyrifos releases on natural aquatic systems is urgently needed.

After release to the natural environment, chlorpyrifos adversely impacts non-target organisms. For instance, different concentrations of chlorpyrifos (18.75, 37.5, 75, and 150 mg/L) significantly inhibited the growth of green algae, and the growth rate decreased gradually with the increase of its concentration (Asselborn et al., 2015). It has been reported that the mortality of *Clarias gariepinus* reached 50% after

* Corresponding author.
E-mail address: hfqian@zjut.edu.cn (H. Qian).

https://doi.org/10.1016/j.ecoenv.2023.115230
Received 3 May 2023; Received in revised form 30 June 2023; Accepted 2 July 2023
Available online 5 July 2023

treatment of 0.5 μg/L chlorpyrifos for 96 h (Woke and Aleleye-Wokoma, 2009). However, most of the previous studies on the impacts of chlorpyrifos on aquatic ecosystems focused on big-size model organisms and ignored the responses of aquatic microorganisms at the community level (Staley et al., 2015). Aquatic microorganisms act as producers, consumers, and decomposers in the aquatic environment, and their contributions to nutrient cycles maintain the stability of aquatic ecosystems (Lu et al., 2019; Schoffelen et al., 2019; Xu et al., 2023; Zhang et al., 2021). Because aquatic microorganisms are sensitive to exogenous contaminants, such as fungicides, herbicides, antibiotics, insecticides, and nanoparticles (Kusi et al., 2020; Qiu et al., 2022; Wang et al., 2023; Zhou et al., 2020), they also play critical roles as indicators of pollutant and aquatic environmental health. Taking advantage of omics biotechnology, we can nowadays explore the composition and specific ecological functions of the microbial community (Xu et al., 2022; Yu et al., 2023). Meanwhile, we can comprehensively assess the ecotoxicity of pollutants caused by anthropogenic interference in the aquatic ecosystem at the more complex microbial community level instead of the simple single-organism level.

In the process that pesticides affect microbial community structure, pesticide-resistant strains can acquire antibiotic resistance under pesticide selection pressure, resulting in pesticide-antibiotic cross-resistance (Rangasamy et al., 2018). Therefore, assessing the impacts of risky antibiotic resistance genes (ARGs) and pathogens threatening human health in aquatic ecosystems under chlorpyrifos exposure is fundamentally essential.

Here, we collected unpolluted freshwater and added zebrafish to construct an aquatic microcosm. We then investigated the effect of chlorpyrifos on the composition and functional potential of the aquatic and zebrafish intestinal microbiomes. The objective of this study was to comprehensively assess the ecological risk of chlorpyrifos to the aquatic environment using 16S rRNA gene sequencing and metagenomics.

2. Materials and methods

2.1. Establishment of freshwater microcosms

A 45 L freshwater samples were collected from an uncontaminated pond (0.5 m depth) at Zhejiang University of Technology, Hangzhou, China (30° 17′45.11″ N, 120° 09′ 50.07″ E) in August 2020, and immediately transferred to the laboratory. Freshwater samples were placed under a 46 E m^{-2} s^{-1} cool-white fluorescent light with a 12:12 h light-to-dark photoperiod at 25 ± 0.5 °C for 3 d for adaptation and settling. Six-month-old zebrafish (*Danio rerio*) were obtained from the China Zebrafish Resource Center (Hubei, China) and acclimated for 7 d in the collected pond water with the same conditions as in the freshwater samples. Chlorpyrifos (powder, 99.6% purity) was obtained from Dr. Ehrenstorfer Co., Ltd (Augsburg, Germany) and dissolved in a concentration of 0.1% in dimethyl sulfoxide (DMSO) The 0.1% concentration of DMSO used in this study was safe for aquatic microbial communities (Qi et al., 2008). Chlorpyrifos concentrations exceeding 0.2 μg/L have been detected in natural water bodies across multiple regions, and the lowest concentration causing slight toxicity to freshwater fish is reported to be 2.1 μg/L (Huang et al., 2020). Therefore, we selected chlorpyrifos treatment concentrations of 0.2 μg/L and 2.0 μg/L. The microcosm experiment comprised two treatment groups, with chlorpyrifos concentrations of 0.2 μg/L and 2.0 μg/L, respectively, along with a control group. Each group was consisted of five biological replicates, with each replicate containing 6 healthy male zebrafish of 6 months old, measuring approximately 3.5 cm in length. The microcosm was constructed by adding 1.8 L of previously collected freshwater and six zebrafish to a sterilized 2 L beaker, followed by treatment with chlorpyrifos. The zebrafish were fed twice daily with zebrafish feed purchased from BIOZYM Co., Ltd., and were alive during the treatment.

2.2. Analysis of water quality parameters in microcosm

Electrical conductivity and pH were measured every two days. The electrical conductivity of the microcosm was determined using an electrical conductivity meter (InPro 7100i/12/120, Meter Toledo®, Columbus, USA), and the pH value was measured with a pH meter (FE-20, Mettler Toledo®, Columbus, USA).

To analyze the total nitrate content in the water, a 2 mL water sample was mixed with 1 mL of alkaline potassium persulfate solution in a test tube. The alkaline potassium persulfate solution consisted of 40 g potassium persulfate and 15 g sodium hydroxide dissolved in 1 L water. The mixture underwent high-temperature digestion for 30 min. Then, 120 μL of hydrochloric acid solution with a mass fraction of 18.4% was added. Absorbance values were measured at 220 nm and 275 nm using a microplate reader. The total nitrate content was determined by comparing the measured values with a standard curve.

To determine the total phosphorus content in the water, a 2 mL water sample was mixed with 200 μL of a 50 g/L potassium sulfite solution in a test tube. The mixture was then subjected to high-temperature digestion for 30 min. Subsequently, 80 μL of 100 g/L ascorbic acid solution was added, followed by the addition of 160 μL of molybdate solution. The molybdate solution was prepared by combining three solutions: diluted concentrated sulfuric acid (30 mL), ammonium molybdate (1.3 g dissolved in 10 mL water), and potassium antimonyl tartrate (0.035 g dissolved in 10 mL water). After allowing the mixture to settle for 15 min, absorbance values were measured at a wavelength of 700 nm using a microplate reader. The total phosphorus content was calculated by comparing the measured values with a standard curve.

2.3. Microcosm metagenome sample preparation and sequencing

Aquatic microorganisms were collected from a 100 mL freshwater sample filtered through a 0.45-μm pore diameter membrane at 0, 7, and 14 d of treatment (control, 0.2 and 2.0 μg/L) by chlorpyrifos and stored at − 80 °C after collection, with three biological replicates of each treatment for metagenome assessment. Total nucleic acids were extracted by E.Z.N.A.® DNA Kit (Omega Bio-tek, USA) according to the manufacturer's instructions and sequenced on the Illumina Hiseq Xten platform (Illumina, San Diego, USA) by Majorbio Bio-Pharm Technology Co., Ltd. (Shanghai, China).

2.4. Microcosm metagenome assembly and analysis

The raw reads acquired from sequencing were filtered using fastp v0.20.0 (http://opengene.org/fastp/) software, and the cleaned reads were assembled into contigs via MEGAHIT v1.1.2 (http://github.com/voutcn/megahit) and resulted in contigs with length ≥ 300 bp for further gene prediction. MetaGene (http://metagene.cb.k.u-tokoyo.ac.jp/) was used to predict the Open reading frames (ORFs) in the contigs and translate ORFs with length ≥ 100 bp into amino acid sequences. We constructed non-redundant gene sets by clustering the predicted genes using CD-HIT (http://www.bioinformatics.org/cd-hit/), with default parameters (90% identity and 90% coverage), selecting the longest sequences from each cluster as representative sequences. High-quality reads were then compared with non-redundant gene sets with 95% identity using SOAPaligner (http://soap.genomics.org.cn/) to acquire information on gene abundance in each sample. The non-redundant gene set was aligned with the NR database using DIAMOND v0.8.17.79 (Buchfink et al., 2021) with an e-value cutoff of $1e^{-5}$, and the species annotation results were obtained from the corresponding taxonomic information database of the NR database. Then the species abundance was calculated using the sum of the corresponding gene abundance of the species. DIAMOND v0.8.17.79 was also applied to align the non-redundant gene sets against the Kyoto Encyclopedia of Genes and Genomes database (KEGG) and the Comprehensive Antibiotic Resistance Database (CARD) (http://arpcard.Mcmaster.ca), with an

e-value cutoff of $1e^{-5}$, to annotate function and identify ARGs. We determine the taxonomic annotation of each ARG-carrying unigene by comparing the species table and the ARG table.

The risk of ARGs caused by chlorpyrifos was evaluated via the workflow established by Zhang et al. (2022b). To evaluate the risks associated with ARGs, four indices, namely "human accessibility" (HA), "mobility" (MO), "human pathogenicity" (HP), and "clinical availability" (CA), were established. The risk index (RI) for each ARG was calculated using the formula: RI = HA × MO × HP × CA. Employing this workflow, all ARGs were ranked based on their calculated risks. The opportunistic human bacterial pathogens (HBPs) were identified by cross-referencing the species table, and a list of potential HBPs was compiled in a previous study (Li et al., 2015).

2.5. 16S rRNA gene sequencing and analysis

To assess the impact of chlorpyrifos exposure (0.2 and 2.0 μg/L) on the gut bacteria of zebrafish, the entire intestines were dissected after 0, 7, and 14 days of exposure (30 samples per group). The dissected samples were immediately frozen using dry ice and stored at − 80 °C until further analysis. All procedures were conducted under sterile conditions. After extraction of total nucleic acid by an E.Z.N.A.® Soil DNA Kit, the V3-V4 regions of bacterial 16S rRNA genes were amplified by a polymerase chain reaction (PCR) thermocycler system (GeneAmp 9700, ABI, USA) using primers 38、F (5′-ACTCCTACGGGAGGCAGCAG-3′) and 806R (5′-GGACTACHVGGGTWTCTAAT-3′). The purified amplicons were then sequenced on an Illumina Miseq PE300 platform (Illumina, San Diego, USA) by Majorbio Bio-Pharm Technology Co., Ltd. (Shanghai, China). The raw reads acquired from sequencing were filtered by fastp software. Next, operational taxonomic units (OTUs) were clustered using UPARSE v7.1 (http://drive5.com/uparse/) with a 97% similarity threshold via a 'greedy' algorithm that performed chimera filtering and OTU clustering simultaneously. Taxonomy was inferred from 16S rRNA gene sequences using an RDP Classifier algorithm (http://rdp.cme.msu.edu/) against the Silva database (Release 138) with a 70% confidence threshold. OTUs and their tags annotated as chloroplasts or mitochondria and cannot be annotated at the kingdom level were removed. The bacterial functions were predicted by the Tax4Fun tool.

2.6. Statistics and visualization

The data were presented as the mean ± standard error mean (SEM) to represent the stability of the mean value across different samples. One-way analysis of variance (ANOVA) was performed using StatView (Version 5.0.1) compare the effects of different concentrations and treatment durations of chlorpyrifos treatment on the microbial structure. Two-tailed *t*-tests were performed in Excel Analysis Tools (Microsoft Corporation, Redmond, USA) to assess the significant differences in microbial abundance between chlorpyrifos treatment and the control group at different concentrations and treatment durations. Values were considered to differ significantly at $p < 0.05$. Alpha diversity indices (Richness and Shannon index) were calculated at the genus level using the vegan package in R. Principal coordinates analysis (PCoA) based on the Bray-Curtis inter-sample distance matrix at the genus level was performed to determine the differences between groups of the microbial community, using the vegan package in R. Volcano plots of genera were generated via the ggplot2 package in R. Random forest classification analysis was performed to identify the microbial biomarkers at the family level between control and treatment groups using the RandomForest package in R. Co-occurrence network analysis was performed to investigate the interactions between the aquatic microbial community in each group based on genera with a mean relative abundance of over 0.1% in all samples and a relative abundance of over 0.5% in any one sample. We calculated the pairwise Spearman's correlation coefficient using the package psych in R, with strong and significant ($r > 0.8$ or $r < -0.8$, $p < 0.05$) correlations retained. We used Gephi v0.9.2 to calculate topological parameters (average degree, clustering coefficient, and modularity) and visualize the co-occurrence network via Cytoscape v3.9.0. Bubble graphs of functions analysis were visualized by the ggplot2 package in R. Heatmaps were constructed via the TBtools v1.0. Other plots were plotted by GraphPad Prism v9.00.

3. Results

3.1. Effects of chlorpyrifos on water quality parameters in microcosm

During the 14-days chlorpyrifos treatments, the pH of the freshwater ranged between 7 and 8.5, exhibiting an upward trend with increasing exposure time in the microcosm ($p < 0.05$; Fig. S1a). The electrical conductivity value increased significantly on 7th and 8th d under 2.0 μg/L chlorpyrifos exposure (Fig. S1b). The total phosphorus and NO_3^--N content increased on 7 d with 2.0 μg/L chlorpyrifos treatment while decreased on 14 d after both two concentrations of chlorpyrifos exposure ($p < 0.05$; Figs. S1c, d). The variations in water quality parameters indicated that chlorpyrifos treatment may disrupt the stability of the aquatic ecosystem.

3.2. Effects of chlorpyrifos on microbial community diversity and structure

The alpha diversity analysis of the microbial community was carried out at the genus level. The richness of the microbial community decreased significantly after 14 d of 2.0 μg/L exposure (two-tailed *t*-test, $p = 0.008$; Fig. 1a). Neither concentration of chlorpyrifos (0.2 and 2.0 μg/L) significantly affected the Shannon index of the microbial community after 14 d of chlorpyrifos treatment (Fig. 1b). PCoA analysis based on Bray-Curtis dissimilarity at the genus level indicated that 0.2 and 2.0 μg/L of chlorpyrifos treatment significantly changed the microbial community composition on 7 d (Adonis analysis, $R^2 = 0.3416$, $p = 0.019$; Fig. 1c and Fig. S2a), but this effect diminished on 14 d (Adonis analysis, $R^2 = 0.1276$, $p = 0.198$; Fig. 1c and Fig. S2b). Nevertheless, the microbial community structure was more distinct from the control under the high concentration (2.0 μg/L) chlorpyrifos treatment than the low (0.2 μg/L) chlorpyrifos treatment.

Bacteria, eukaryota, archaea, and viruses accounted for 94.2%, 3.8%, 0.3%, and 1.6% of the microbial community in freshwater, respectively (Fig. 1d). Compared with the control, the abundance of 71 and 95 genera were significantly changed with the treatment of 0.2 μg/L chlorpyrifos on 7 and 14 d, respectively (two-tailed *t*-test, $p < 0.05$; Figs. S3a, b). And the abundance of 83 and 327 genera were significantly changed with the treatment of 2.0 μg/L chlorpyrifos on 7 and 14 d, respectively (two-tailed *t*-test, $p < 0.05$; Figs. S3c, d). The variations in abundance of genera showed that increasing chlorpyrifos concentrations and time exacerbated the negative impacts on the aquatic microbial community. Analysis of the bacterial composition at the phylum level showed that Proteobacteria, Bacteroidetes, and Actinobacteria were the dominant bacteria phyla. Compared with the control, the treatment of 2.0 μg/L chlorpyrifos decreased the relative abundance of Proteobacteria, with opposite effects on Bacteroidetes after 7 d of exposure. After the 14-d treatment of both concentrations of chlorpyrifos, the relative abundance of Acidobacteria decreased (two tailed *t*-test, $p < 0.05$; Fig. 1e and Fig. S4). We constructed a classification model using the random forest algorithm to determine biomarkers at the family level that can distinguish microbial communities in groups with or without chlorpyrifos treatments, and 39 families (mean decrease accuracy > 1.0) were more sensitive to chlorpyrifos treatment. Most of them belonged to Proteobacteria (n = 15), Actinobacteria (n = 5), and Bacteroidetes (n = 4), and only 15 families presented a relative abundance > 0.1% (Fig. S5). The relative abundance of some families that contained pathogenic genera was increased by chlorpyrifos treatment, such as *Mycobacteriaceae* and *Enterobacteriaceae*.

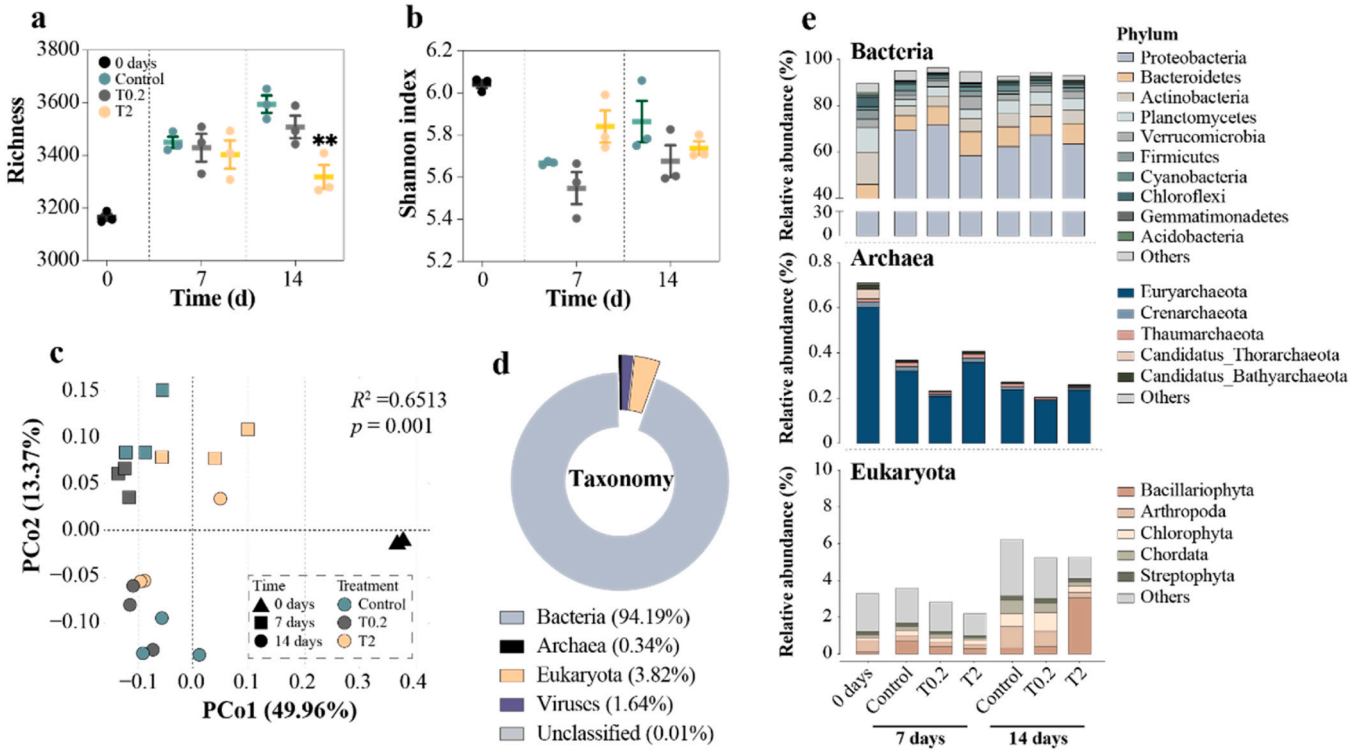

Fig. 1. Effects of chlorpyrifos on diversity and structure of microbial communities. a, b Richness and Shannon index of microbial communities calculated at the genus level. * represents a significant difference between the control and the chlorpyrifos treatments (two tailed *t*-test, $p < 0.05$). c Principal coordinates analysis (PCoA) based on the Bray-Curtis distance coefficient of the microbial community at genus level after chlorpyrifos treatment. d Taxonomic composition of the microbial community in all samples. **e** Effects of chlorpyrifos on the bacteria (top 10), archaea (top 5), and eukaryote (top 5) community composition at the phylum level.

The composition of archaea showed that Euryarchaeota was the dominant phyla, and its relative abundance decreased in the 0.2 μg/L of chlorpyrifos treatment after 7 d, while the relative abundance of Thaumarchaeota decreased after the 14-d treatment of both concentrations of chlorpyrifos (two tailed *t*-test, $p < 0.05$; Fig. 1e and Figs. S6a, b). A significantly decreased relative abundance was found in

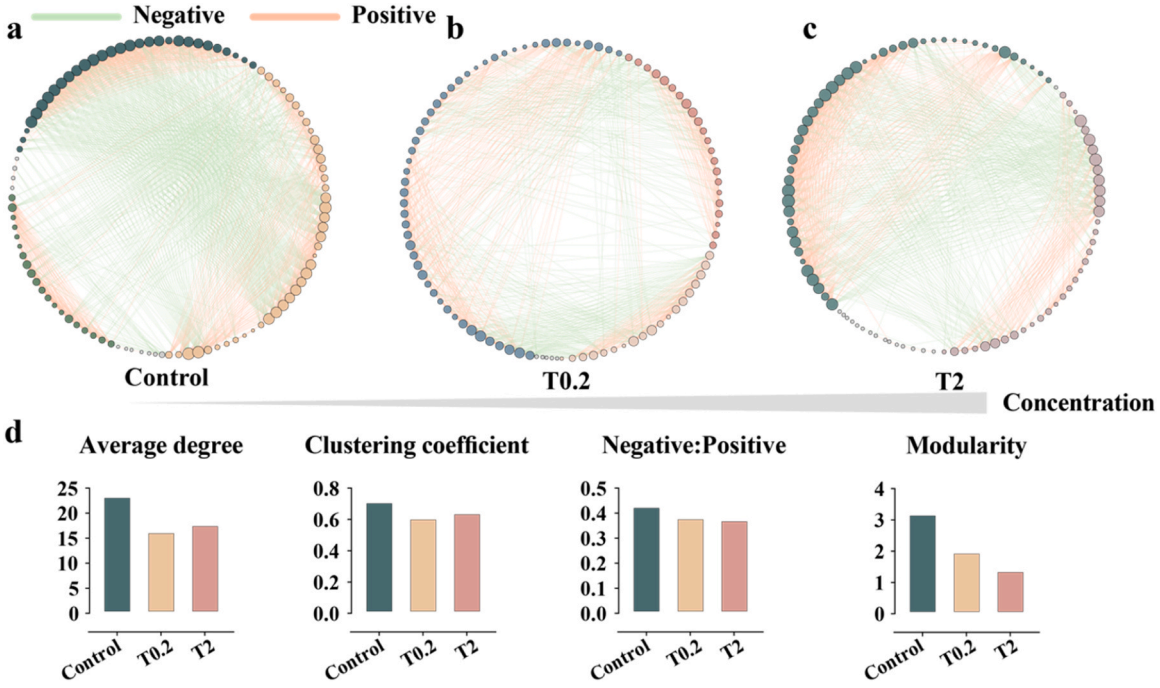

Fig. 2. Effects of chlorpyrifos on microbial co-occurrence networks at the genus level. a-c Co-occurrence network among genera in the control (a) and 0.02 (b) and 0.2 (c) μg/L of chlorpyrifos treatments. Nodes are colored according to the module, modules with fewer than five nodes are gray, and node size represents the number of connections. d Topological parameters (average degree, clustering coefficient, negative and positive edges ratio, and modularity) of microbial interaction networks.

Arthropoda and Chordata belonged to the eukaryota after 2.0 μg/L of chlorpyrifos treatment on 14 d (two tailed *t*-test, $p < 0.05$; Fig. 1e and Figs. S6c, d).

Co-occurrence networks were constructed to explore the relationship among genera under the chlorpyrifos treatments. After filtering out non-significantly correlated nodes ($|r| > 0.8$, $p < 0.05$), we obtained a total of 102, 96, and 98 nodes in the control, 0.2 μg/L chlorpyrifos treatment, and 2.0 μg/L chlorpyrifos treatment, respectively. These nodes formed 1194 edges (512 negative and 682 positive), 785 edges (301 negative and 484 positive), and 872 edges (327 negative and 546 positive) in the respective treatments (Fig. 2a-c). Decreases existed in the average degree and clustering coefficient after chlorpyrifos treatments, and these topological parameters slightly recovered with increased chlorpyrifos concentration but were still much lower than the control (Fig. 2d). The ratio of negative and positive and modularity decreased after both concentrations of chlorpyrifos treatments (Fig. 2d).

3.3. Effects of chlorpyrifos on microbial community function

Based on KEGG database annotation, chlorpyrifos treatment significantly affected the functional potential of aquatic microorganisms, including functions related to organic degradation, element cycling, and energy flow in aquatic ecosystems. The abundance of 23 and 13 functional genes significantly changed under 0.2 μg/L chlorpyrifos treatment on 7 d and 14 d, respectively, while the abundance of 31 and 77 functional genes significantly changed under 2.0 μg/L chlorpyrifos treatment on 7 d and 14 d, respectively (two tailed *t*-test, $p < 0.05$; Fig. 3a). After 14 d of 0.2 μg/L chlorpyrifos treatment, most functional pathways recovered ($|\log_2(\text{fold change})| = 0$), whereas after 14 d of 2.0 μg/L chlorpyrifos treatment, most functional pathways exhibited a downregulated state ($\log_2(\text{fold change}) < 1$, Fig. 3a), which paralleled the trend observed in the microbial community composition (Fig. S3). Specifically, functions associated with metabolism pathways, such as metabolism of terpenoids and polyketides, and glycan biosynthesis increased, whereas no functions associated with environmental information processes and cellular processes changed sharply ($|\log_2(\text{fold change})| < 1$) after 7 d of chlorpyrifos treatment (Fig. S7). In contrast, almost all functions associated with environmental information processing (signal transduction and signaling molecules and interaction), cellular processed (cell motility and cellular community-

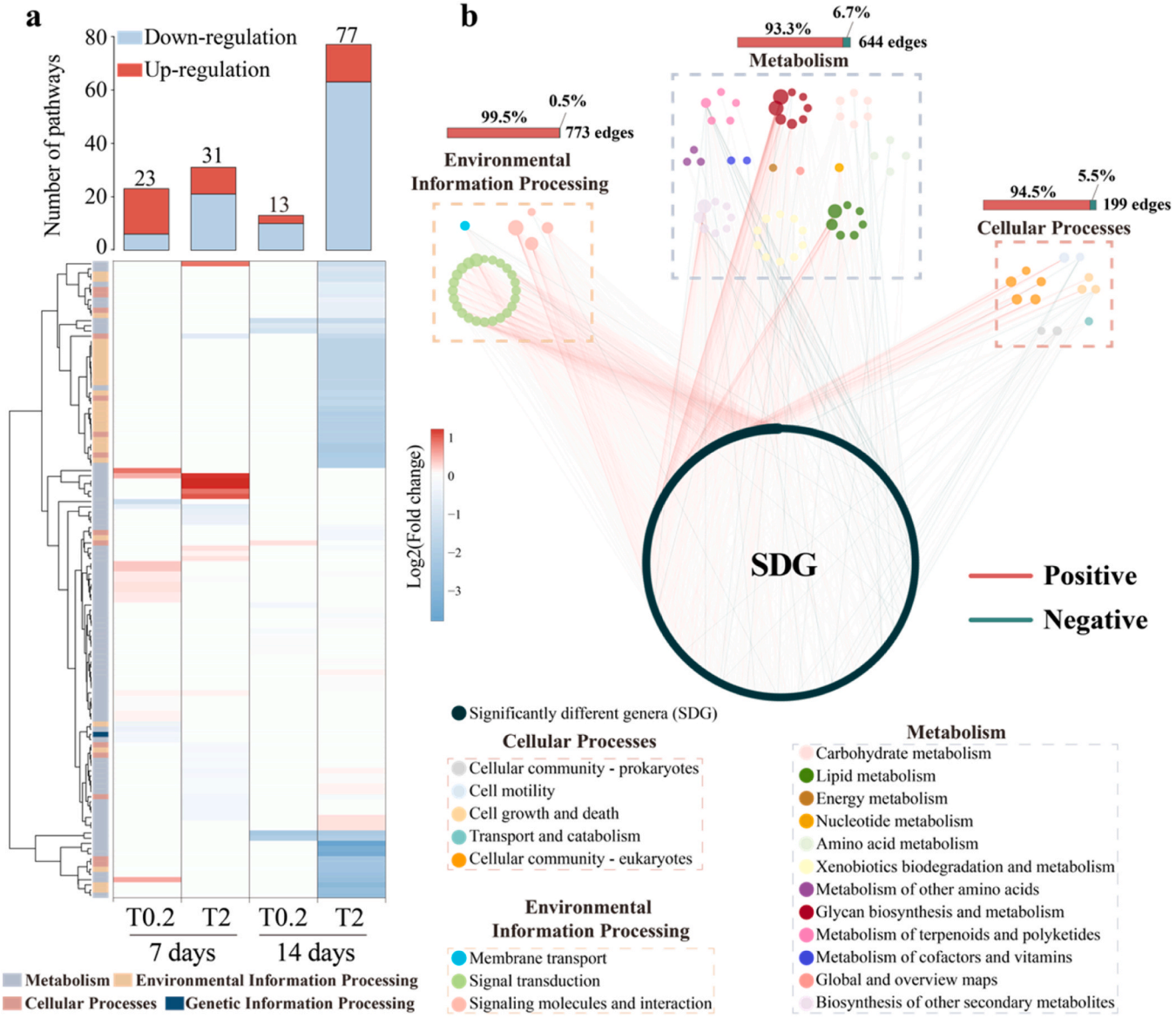

Fig. 3. Effects of chlorpyrifos on the functions of microbial communities. a Heatmap of pathways significantly changed ($p < 0.05$) under different chlorpyrifos treatments after 7 and 14 d. b Relationships between significantly changed genera and functional pathways. Node size represents the number of connections.

eukaryotes), and metabolism (lipid metabolism, metabolism of terpenoids and polyketides, glycan biosynthesis and metabolism, and biosynthesis of other secondary metabolites) decreased after 14 d of chlorpyrifos treatment (Fig. S7). The variations in microbial functional abundance indicated that higher concentrations of chlorpyrifos treatment increased the negative impact on the functional potential of water microbial communities compared to lower concentrations. Furthermore, this negative impact became more persistent over time, making recovery more challenging.

We constructed a co-occurrence network based on the significantly different genera and functions. Nearly all the significantly different genera exhibited a positive correlation with functions related to environmental information processing, cellular processing, and metabolism (Fig. 3b). This finding confirmed the common trend of changes in genera and functions after chlorpyrifos treatment, indicating that chlorpyrifos could affect the microbial composition and, thus, microbial functioning.

3.4. Effects of chlorpyrifos on human pathogenic bacteria and ARGs

In total, 622 ARGs classified into 25 types were identified in all samples, and most of them belonged to multidrug, beta-lactams, and aminoglycoside antibiotics (Fig. S8). According to the assessment of ARGs by Zhang et al. (2022b), we identified 247 risky ARGs mainly classified as multidrug, tetracycline, and aminoglycoside antibiotic, and found that both concentrations of chlorpyrifos treatment significantly increased the number of risky ARGs after 7 d of exposure (two tailed *t*-test, $p < 0.05$; Figs. S9a, b).

Based on the pathogenic bacteria list, we identified 402 opportunistic HBPs in all groups. We selected 70 HPBs which were significantly changed under chlorpyrifos treatment for the subsequent analysis. A total of 32 antibiotic-resistant pathogens, such as *Pseudomonas fluorescens*, *Ralstonia pickettii*, and *Pseudomonas stutzeri*, which were also the most abundant, were obtained by comparing the taxonomic information of ARGs (Fig. 4a). With the increase in the concentration of chlorpyrifos, the number of HPBs significantly enriched increased on 7 and 14 d (Fig. 4b). The co-occurrence network analysis of ARGs and microbiome focused on risky ARGs and HPBs and revealed that most HPBs showed positive correlations with risky ARGs (Fig. 4c). This indicates a potential threat for human health when chlorpyrifos is released into the aquatic environment.

3.5. Effects of chlorpyrifos on zebrafish intestinal microbial community

We used 16S rRNA gene sequencing to analyze the zebrafish intestinal microbial community change after chlorpyrifos treatment. At the end of the chlorpyrifos treatment for 14 d, alpha diversity (Shannon index and Richness) exhibited no significant difference compared with the control, except for a decrease in microbial community richness after 7 d of exposure (Fig. 5a). The PCoA with Bray-Curtis dissimilarity at the genus level on 7 and 14 d also exhibited no significant effect on the microbial community structure (Fig. 5b, c). The microbial community composition at the genus level was disturbed by chlorpyrifos (Fig. 5d). The functional prediction by the Tax4Fun tool revealed that chlorpyrifos mostly regulated the functions associated with metabolism at a low concentration (0.2 μg/L) after 7 d, albeit to a low degree ($|\log_2(\text{fold change})| < 1$), but reverted after 14 d (Fig. 5e). The high concentration (2.0 μg/L) of chlorpyrifos had a slight effect on zebrafish intestinal microbial community functioning.

4. Discussion

With the wide application of chlorpyrifos in agriculture, it is inevitably released into freshwater environments. Therefore, assessing the environmental risks of contamination by chlorpyrifos for freshwater ecosystems is urgent. In this research, we constructed freshwater microcosms and evaluated the effects of chlorpyrifos contamination on microbial communities via metagenome and 16S rRNA gene sequencing.

The structure of microbial community is closely related to the ability of the microorganisms to cope with exogenous stress (Ma et al., 2022). When xenobiotic compounds enter the environmental survival conditions, microbial communities can maintain their diversity via redundancy effects to deal with environmental perturbations (Allison and

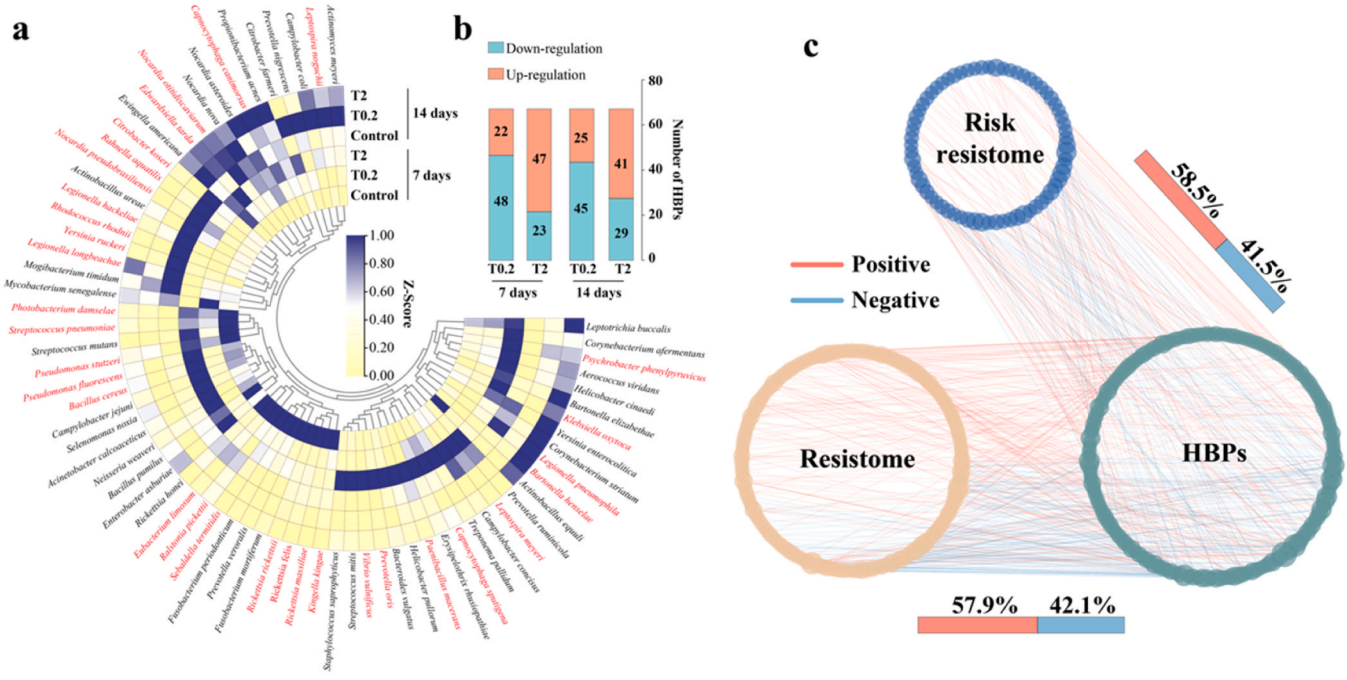

Fig. 4. Effects of chlorpyrifos on the composition of human bacterial pathogens and antibiotic resistome. a The composition of human bacterial pathogens (HBPs) in all groups significantly changed under different chlorpyrifos treatments after 7 and 14 d. Antibiotic-resistant pathogens (ARPs) are marked in red. b The number of HBPs significantly changed after 7 and 14 d treatments of chlorpyrifos. **c** Relationships between HBPs and antibiotic resistome in the aquatic microbial community. Node size represents the number of connections.

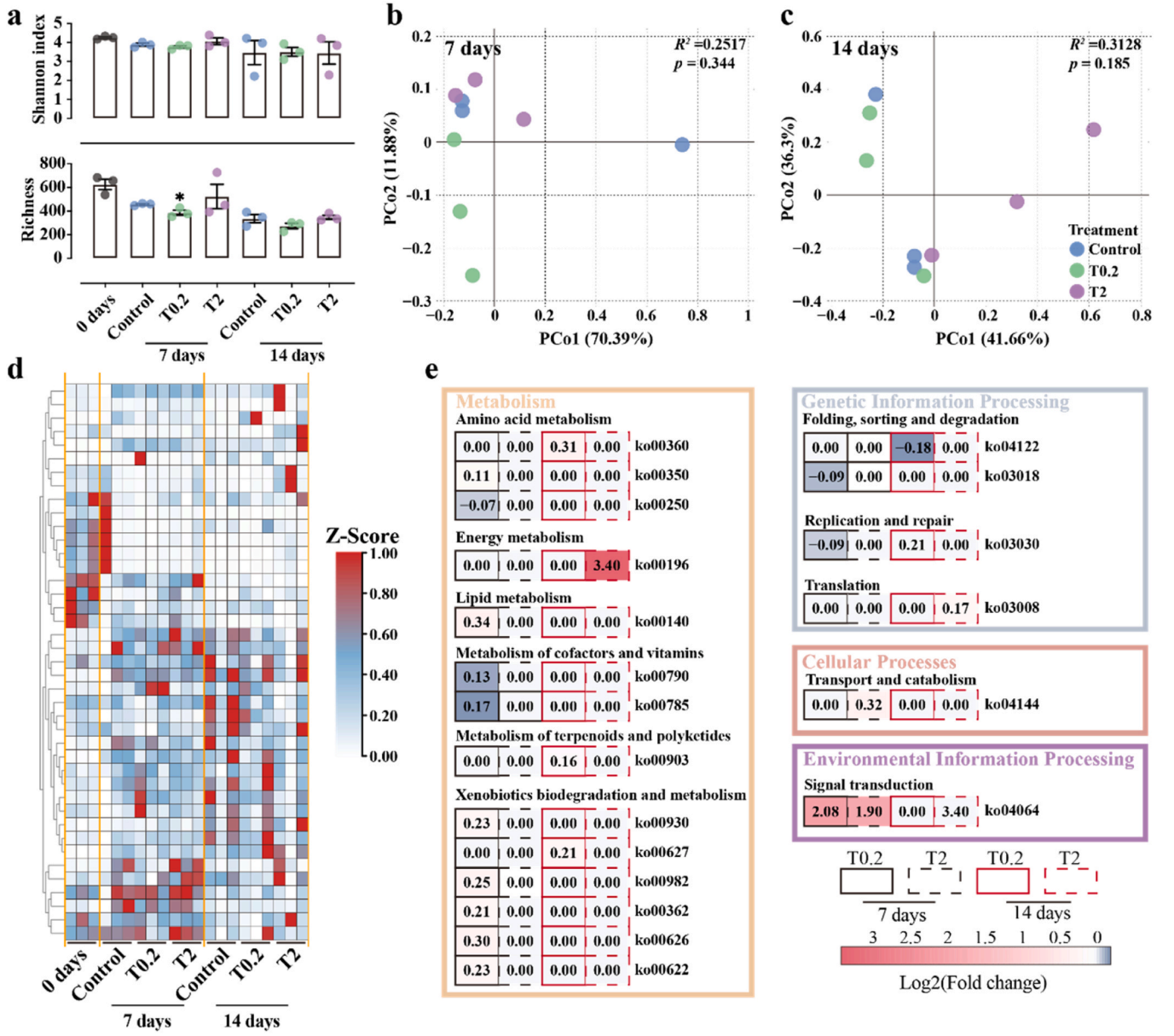

Fig. 5. Effects of chlorpyrifos on zebrafish intestinal microbial community. a Richness and Shannon index of zebrafish intestinal microbial community calculated at the genus level. * represents a significant difference between the control and the chlorpyrifos treatments (two tailed *t*-test, $p < 0.05$). b, c Principal coordinates analysis (PCoA) based on the Bray-Curtis distance coefficient of the zebrafish intestinal microbial community at the genus level under chlorpyrifos treatment 7 (b) and 14 d (c). d Taxonomic composition of zebrafish intestinal microbial community at genus level in all samples. e Effects of chlorpyrifos on KEGG level-3 pathways of the zebrafish intestinal microbial community. Pathways significantly changed ($p < 0.05$) are shown.

Martiny, 2008; Louca et al., 2018). However, in our study, we observed that the diversity and composition of the microbial community were disturbed under chlorpyrifos treatment, and the number of significantly different genera increased over time and concentrations, especially downregulated genera. This suggests that the pressure from chlorpyrifos has exceeded the ability of the microbiome to adapt. Pollutants generate selective pressures to promote the growth of potentially degrading microorganisms, thereby degrading pollutants and reducing pollution pressures (Okoye et al., 2020). For example, *Rhodobacter* and *Acidovorax*, which can degrade organophosphorus pesticides (Ning et al., 2010; Wu et al., 2019), were enriched upon exposure of the microbial community to 0.2 μg/L chlorpyrifos. This indicates that aquatic microorganisms were activated to resist exogenous chlorpyrifos. However, the enrichment phenomenon diminished after the 2.0 μg/L chlorpyrifos treatment, potentially due to the disruption of the function of microbial community, surpassing its overall capacity to regulate or resist chlorpyrifos.

Co-occurrence network analysis contributes to comprehending potential interactions between microorganisms in the environment that coexist with chlorpyrifos. The modular structure of complex microbial networks contributes to their function and community stability (Liu et al., 2019). Our study found complex microbial network structures and modular associations with strong interactions between microorganisms. However, compared with the control, decreases were observed in the number of nodes and edges of the microbial co-occurrence network. This suggests that chlorpyrifos disturbed the aquatic microbial community and reduced the co-occurrence complexity. This might be the consequence of increases in selective pressures (Han et al., 2022). In complex microbial ecological networks, microorganisms interact with each other and exchange matter and energy and resist multifarious external

pressures (Xun et al., 2019; Yuan et al., 2021). The whole microbial community needs to maintain feedback loops formed by microbial interactions, and external disturbances experienced by any member of these loops quickly propagate throughout the system (Coyte et al., 2015). Negative interactions can induce negative feedback loops, which can resist the perturbation experienced by both its own members and the associated positive feedback loops to maintain community stability (Fontaine et al., 2011). Low modularity indicates that cross-module correlation among taxa is common, which leads to a perturbation effect on taxa in one module being more easily propagated to other modules in the face of external pressure, resulting in the instability of the community (Hernandez et al., 2021). Therefore, the decrease in the ratio of negative to positive links and modularity indicated that chlorpyrifos destabilized the aquatic microbial community. The analysis of the random forest algorithm revealed that most families sensitive to chlorpyrifos were at a low-level abundance, indicating that rare taxa may be essential to maintain the stability of the microbial community under chlorpyrifos treatment. Rare taxa play a more critical role in microbial networks than abundant taxa (Xue et al., 2018).

Chlorpyrifos treatments interfered with the aquatic microbial functional potential, which is perhaps a consequence of the disturbance of the aquatic microbial community structure by chlorpyrifos. This was further explained by the apparent positive correlations between the significantly changed genera and functions. Microbial communities play an essential role as mediators in vital ecosystem processes such as organic matter degradation and detoxification of organic pollutants (Widenfalk et al., 2008). Changes in microbial community structure may disturb these functions when microbial communities cannot compensate for the loss of functions relevant to chlorpyrifos-sensitive microorganisms through functional redundancy (Muturi et al., 2017). After 14 d of chlorpyrifos treatment, most functions associated with signal transduction and signaling molecules, as well as their interaction decreased. Microbial signaling responses are generally induced to detoxify contaminants as a buffer against biotic and abiotic pressures (Bickerton et al., 2016; Dufrêne and Persat, 2020). Overall, this suggests that chlorpyrifos treatment reduces the ability of microorganisms to resist stress. Besides, the major functions of metabolism (such as lipid metabolism, glycan biosynthesis and metabolism, and biosynthesis of other secondary metabolites) were obviously downregulated, which were the basis for the survival and activity of microorganisms (Zhang et al., 2022a). These findings indicated that changes in microbial community functions probably further affect the ecological function of the aquatic ecosystems.

Of 622 ARGs detected in our study, 39.7% (247) were considered a threat to human health, and an increase in the number of risky ARGs was observed following treatment with chlorpyrifos. Similarly, in the pathogens we detected, the number of significantly upregulated pathogens increased as the chlorpyrifos concentration increased, which may pose a potential threat to aquatic ecosystems and human health. Pathogens with these risky ARGs are of particular concern (Sun et al., 2022). For instance, *Klebsiella oxytoca* and *Bacillus cereus*, which belong to *Enterobacteriaceae* and *Bacillaceae*, respectively, are both enriched after chlorpyrifos treatment. There have been outbreaks of antibiotic-resistant *Klebsiella oxytoca* in hospitals worldwide, which have been reported to be resistant to colistin (Jayol et al., 2015) and carbapenem (Leitner Eva et al., 2014). It has been reported that *Bacillus cereus*, which causes a minority of foodborne illnesses, can generate resistance to erythromycin, tetracycline, and carbapenem (Kiyomizu et al., 2008; Kotiranta et al., 2000; Savini et al., 2009). Additionally, our study observed that most pathogens were positively correlated with risky ARGs. The promotion of their growth by chlorpyrifos was undoubtedly a threat to aquatic ecosystems and human health. This is to be concluded despite the fact that we do not have direct evidence for mobility or lateral transfer of ARGs in our study. A previous study showed that chlorpyrifos could produce reactive oxygen species (ROS) to damage cell membranes and increase their permeability, probably promoting the horizontal transfer of ARGs (Shahid et al., 2021).

Unlike the aquatic microbial community, chlorpyrifos had only a slight effect on the intestinal microbial community composition and structure of the zebrafish. This suggests that the zebrafish intestinal microbial community was resilient to the invasion of chlorpyrifos. Host health is strongly associated with a robust intestinal microbial community, as it influences the health of the host by regulating the absorption and metabolism of nutrients and stimulating the immune response of the host (Sommer et al., 2017; Tang et al., 2021). The main up-regulated functions included signal transduction, lipid metabolism, and xenobiotics biodegradation and metabolism, all of which are essential for microorganisms to degrade exogenous pollutants (Kim et al., 2015). This indicates that the self-regulation ability of the intestinal microbial community of zebrafish to degrade pollutants was promoted by this treatment. However, the inhibition in the metabolism of cofactors and vitamins indicated that chlorpyrifos might cause intestinal metabolic disorders (Qiao et al., 2019). These results indicated that the effect of chlorpyrifos on the intestinal microbial community of zebrafish was more reflected at the functional level.

5. Conclusion

In summary, our study aimed to investigate the effects of chlorpyrifos exposure on diversity, composition, and functions of microbial community in freshwater ecosystems, distinguishing itself from previous research that primarily focuses on soil environments or toxicity assessment of individual organisms. Our results demonstrated that chlorpyrifos could disturb the freshwater microbial community structure and composition at concentrations of 0.2 and 2.0 μg/L. Chlorpyrifos is found to be able to destroy the stability of the microbial community and inhibits its capability for environmental information processing and metabolism, especially at the concentration of 2.0 μg/L. Chlorpyrifos treatment increased the number of risky ARGs and enriched some potential pathogens with risky ARGs. In addition, the intestinal microbial community structure of zebrafish can adapt to the pressure of chlorpyrifos and recover to the level of control. This work provided new perspectives for assessing the ecological risk of chlorpyrifos in aquatic ecosystems, specifically focusing on the microbial community, and contributed to the theoretical basis for the rational use of chlorpyrifos to protect aquatic ecosystems.

CRediT authorship contribution statement

Nuohan Xu: Methodology, Investigation, Writing – original draft, Writing – review & editing. **Zhigao Zhou:** Data analysis, Data collection, Experiment, **Bingfeng Chen:** Data analysis, Data collection. **Zhenyan Zhang:** Investigation, Methodology, **Jinfeng Zhang:** Investigation, Experiment, **Yan Li:** Data collection, Validation, **Tao Lu:** Software, **Liwei Sun:** Experiment, **W.J.G.M. Peijnenburg:** Writing - Review & Editing, **Haifeng Qian:** Conceptualization, Writing - Review & Editing, Funding acquisition.

Declaration of Competing Interest

The authors declare that they have no known competing financial interests or personal relationships that could have appeared to influence the work reported in this paper.

Data Availability

Data will be made available on request.

Acknowledgments

This work was financially supported by the National Key Research and Development Program of China (2021YFA0909504 and

2022YFD1700401), the National Natural Science Foundation of China (21976161 and 21777144), and the Zhejiang Provincial Natural Science Foundation of China (LZ23B070001).

Appendix A. Supporting information

Supplementary data associated with this article can be found in the online version at doi:10.1016/j.ecoenv.2023.115230.

References

Allison, S.D., Martiny, J.B.H., 2008. Resistance, resilience, and redundancy in microbial communities. Proc. Natl. Acad. Sci. 105, 11512–11519.

Asselborn, V., Fernández, C., Zalocar, Y., Parodi, E.R., 2015. Effects of chlorpyrifos on the growth and ultrastructure of green algae, *Ankistrodesmus gracilis*. Ecotoxicol. Environ. Saf. 120, 334–341.

Bickerton, P., Sello, S., Brownlee, C., Pittman, J.K., Wheeler, G.L., 2016. Spatial and temporal specificity of Ca^{2+} signalling in *Chlamydomonas reinhardtii* in response to osmotic stress. N. Phytol. 212, 920–933.

Buchfink, B., Reuter, K., Drost, H.-G., 2021. Sensitive protein alignments at tree-of-life scale using DIAMOND. Nat. Methods 18, 366–368.

Caminade, C., McIntyre, K.M., Jones, A.E., 2019. Impact of recent and future climate change on vector-borne diseases. Ann. N. Y. Acad. Sci. 1436, 157–173.

Coyte, K.Z., Schluter, J., Foster, K.R., 2015. The ecology of the microbiome: networks, competition, and stability. Science 350, 663–666.

Dufrêne, Y.F., Persat, A., 2020. Mechanomicrobiology: how bacteria sense and respond to forces. Nat. Rev. Microbiol. 18, 227–240.

Echeverri-Jaramillo, G., Jaramillo-Colorado, B., Sabater-Marco, C., Castillo-López, M.-Á., 2021. Cytotoxic and estrogenic activity of chlorpyrifos and its metabolite 3, 5, 6-trichloro-2-pyridinol. Study Mar. yeasts Potential Toxic. Indic. Ecotoxicol. 30, 104–117.

Fontaine, C., Guimarães Jr, P.R., Kéfi, S., Loeuille, N., Memmott, J., van der Putten, W. H., van Veen, F.J.F., Thébault, E., 2011. The ecological and evolutionary implications of merging different types of networks. Ecol. Lett. 14, 1170–1181.

Han, L., Xu, M., Kong, X., Liu, X., Wang, Q., Chen, G., Xu, K., Nie, J., 2022. Deciphering the diversity, composition, function, and network complexity of the soil microbial community after repeated exposure to a fungicide boscalid. Environ. Pollut. 312, 120060.

Hernandez, D.J., David, A.S., Menges, E.S., Searcy, C.A., Afkhami, M.E., 2021. Environmental stress destabilizes microbial networks. ISME J. 15, 1722–1734.

Hossain, M.S., Chowdhury, M.A.Z., Pramanik, Md.K., Rahman, M.A., Fakhruddin, A.N. M., Alam, M.K., 2015. Determination of selected pesticides in water samples adjacent to agricultural fields and removal of organophosphorus insecticide chlorpyrifos using soil bacterial isolates. Appl. Water Sci. 5, 171–179.

Huang, X., Cui, H., Duan, W., 2020. Ecotoxicity of chlorpyrifos to aquatic organisms: a review. Ecotoxicol. Environ. Saf. 200, 110731.

Huang, Y., Zhang, W., Pang, S., Chen, J., Bhatt, P., Mishra, S., Chen, S., 2021. Insights into the microbial degradation and catalytic mechanisms of chlorpyrifos. Environ. Res. 194, 110660.

Jayol, A., Poirel, L., Villegas, M.-V., Nordmann, P., 2015. Modulation of mgrB gene expression as a source of colistin resistance in *Klebsiella oxytoca*. Int. J. Antimicrob. Agents 46, 108–110.

John, E.M., Shaike, J.M., 2015. Chlorpyrifos: pollution and remediation. Environ. Chem. Lett. 13, 269–291.

Kim, H.-S., Lee, B.-Y., Won, E.-J., Han, J., Hwang, D.-S., Park, H.G., Lee, J.-S., 2015. Identification of xenobiotic biodegradation and metabolism-related genes in the copepod *Tigriopus japonicus* whole transcriptome analysis. Mar. Genom. 24, 207–208.

Kiyomizu, K., Yagi, T., Yoshida, H., Minami, R., Tanimura, A., Karasuno, T., Hiraoka, A., 2008. Fulminant septicemia of *Bacillus cereus* resistant to carbapenem in a patient with biphenotypic acute leukemia. J. Infect. Chemother. 14, 361–367.

Kotiranta, A., Lounatmaa, K., Haapasalo, M., 2000. Epidemiology and pathogenesis of *Bacillus cereus* infections. Microbes Infect. 2, 189–198.

Kusi, J., Scheuerman, P.R., Maier, K.J., 2020. Emerging environmental contaminants (silver nanoparticles) altered the catabolic capability and metabolic fingerprinting of microbial communities. Aquat. Toxicol. 228, 105633.

Leitner, Eva, Gernot, Zarfel, Josefa, Luxner, Kathrin, Herzog, Pekard-Amenitsch, Shiva, Martin, Hoenigl, Thomas, Valentin, Gebhard, Feierl, Grisold, Andrea J., Christoph, H.ögenauer, Heinz, Sill, Robert, Krause, Zollner-Schwetz, Ines, 2014. Contaminated handwashing sinks as the source of a clonal outbreak of KPC-2-producing *Klebsiella oxytoca* on a hematology ward. Antimicrob. Agents Chemother. 59, 714–716.

Li, B., Ju, F., Cai, L., Zhang, T., 2015. Profile and fate of bacterial pathogens in sewage treatment plants revealed by high-throughput metagenomic approach. Environ. Sci. Technol. 49, 10492–10502.

Liu, L., Chen, H., Liu, M., Yang, J.R., Xiao, P., Wilkinson, D.M., Yang, J., 2019. Response of the eukaryotic plankton community to the cyanobacterial biomass cycle over 6 years in two subtropical reservoirs. ISME J. 13, 2196–2208.

Louca, S., Polz, M.F., Mazel, F., Albright, M.B.N., Huber, J.A., O'Connor, M.I., Ackermann, M., Hahn, A.S., Srivastava, D.S., Crowe, S.A., Doebeli, M., Parfrey, L.W., 2018. Function and functional redundancy in microbial systems. Nat. Ecol. Evol. 2, 936–943.

Lu, T., Zhang, Q., Lavoie, M., Zhu, Y., Ye, Y., Yang, J., Paerl, H.W., Qian, H., Zhu, Y.-G., 2019. The fungicide azoxystrobin promotes freshwater cyanobacterial dominance through altering competition. Microbiome 7, 128.

Ma, Q., Tan, H., Song, J., Li, M., Wang, Z., Parales, R.E., Li, L., Ruan, Z., 2022. Effects of long-term exposure to the herbicide nicosulfuron on the bacterial community structure in a factory field. Environ. Pollut. 307, 119477.

Malakootian, M., Shahesmaeili, A., Faraji, M., Amiri, H., Silva Martinez, S., 2020. Advanced oxidation processes for the removal of organophosphorus pesticides in aqueous matrices: a systematic review and meta-analysis. Process Saf. Environ. Prot. 134, 292–307.

Muturi, E.J., Donthu, R.K., Fields, C.J., Moise, I.K., Kim, C.-H., 2017. Effect of pesticides on microbial communities in container aquatic habitats. Sci. Rep. 7, 44565.

Ning, J., Bai, Z., Gang, G., Jiang, D., Hu, Q., He, J., Zhang, H., Zhuang, G., 2010. Functional assembly of bacterial communities with activity for the biodegradation of an organophosphorus pesticide in the rape phyllosphere. FEMS Microbiol. Lett. 306, 135–143.

Okoye, A.U., Chikere, C.B., Okpokwasili, G.C., 2020. Isolation and characterization of hexadecane degrading bacteria from oil- polluted soil in Gio Community, Niger Delta, Nigeria. Sci. Afr. 9, e00340.

Qi, W., Ding, D., Salvi, R.J., 2008. Cytotoxic effects of dimethyl sulphoxide (DMSO) on cochlear organotypic cultures. Hear Res 236, 52–60.

Qiao, R., Sheng, C., Lu, Y., Zhang, Y., Ren, H., Lemos, B., 2019. Microplastics induce intestinal inflammation, oxidative stress, and disorders of metabolome and microbiome in zebrafish. Sci. Total Environ. 662, 246–253.

Qiu, D., Ke, M., Zhang, Q., Zhang, F., Lu, T., Sun, L., Qian, H., 2022. Response of microbial antibiotic resistance to pesticides: an emerging health threat. Sci. Total Environ. 850, 158057.

Rangasamy, K., Athiappan, M., Devarajan, N., Samykannu, G., Parray, J.A., Aruljothi, K. N., Shameem, N., Alqarawi, A.A., Hashem, A., Abd_Allah, E.F., 2018. Pesticide degrading natural multidrug resistance bacterial flora. Microb. Pathog. 114, 304–310.

Rohr, J.R., Barrett, C.B., Civitello, D.J., Craft, M.E., Delius, B., DeLeo, G.A., Hudson, P.J., Jouanard, N., Nguyen, K.H., Ostfeld, R.S., Remais, J.V., Riveau, G., Sokolow, S.H., Tilman, D., 2019. Emerging human infectious diseases and the links to global food production. Nat. Sustain. 2, 445–456.

Savini, V., Favaro, M., Fontana, C., Catavitello, C., Balbinot, A., Talia, M., Febbo, F., D'Antonio, D., 2009. *Bacillus cereus* heteroresistance to carbapenems in a cancer patient. J. Hosp. Infect. 71, 288–290.

Schoffelen, N.J., Mohr, W., Ferdelman, T.G., Duerschlag, J., Littmann, S., Ploug, H., Kuypers, M.M.M., 2019. Phosphate availability affects fixed nitrogen transfer from diazotrophs to their epibionts. ISME J. 13, 2701–2713.

Shahid, M., Manoharadas, S., Altaf, M., Alrefaei, A.F., 2021. Organochlorine pesticides negatively influenced the cellular growth, morphostructure, cell viability, and biofilm-formation and phosphate-solubilization activities of *Enterobacter cloacae* Strain EAM 35. ACS Omega 6, 5548–5559.

Sharma, A., Kumar, V., Shahzad, B., Tanveer, M., Sidhu, G.P.S., Handa, N., Kohli, S.K., Yadav, P., Bali, A.S., Parihar, R.D., Dar, O.I., Singh, K., Jasrotia, S., Bakshi, P., Ramakrishnan, M., Kumar, S., Bhardwaj, R., Thukral, A.K., 2019. Worldwide pesticide usage and its impacts on ecosystem. SN Appl. Sci. 1, 1446.

Sommer, F., Anderson, J.M., Bharti, R., Raes, J., Rosenstiel, P., 2017. The resilience of the intestinal microbiota influences health and disease. Nat. Rev. Microbiol. 15, 630–638.

Staley, Z.R., Harwood, V.J., Rohr, J.R., 2015. A synthesis of the effects of pesticides on microbial persistence in aquatic ecosystems. Crit. Rev. Toxicol. 45, 813–836.

Starner, K., Spurlock, F., Gill, S., Goh, K., Feng, H., Hsu, J., Lee, P., Tran, D., White, J., 2005. Pesticide residues in surface water from irrigation-season monitoring in the San Joaquin Valley, California, USA. Bull. Environ. Contam. Toxicol. 74, 920–927.

Sumon, K.A., Rashid, H., Peeters, E.T., Bosma, R.H., Van den Brink, P.J., 2018. Environmental monitoring and risk assessment of organophosphate pesticides in aquatic ecosystems of north-west Bangladesh. Chemosphere 206, 92–100.

Sun, J., Lin, Z., Ning, D., Wang, H., Zhang, Z., He, Z., Zhou, J., 2022. Functional microbial community structures and chemical properties indicated mechanisms and potential risks of urban river eco-remediation. Sci. Total Environ. 803, 149868.

Tang, J., Wang, W., Jiang, Y., Chu, W., 2021. Diazinon exposure produces histological damage, oxidative stress, immune disorders and gut microbiota dysbiosis in crucian carp (*Carassius auratus gibelio*). Environ. Pollut. 269, 116129.

Wang, Y., Ni, K., Zhang, Z., Xu, N., Lei, C., Chen, B., Zhang, Q., Sun, L., Chen, Y., Lu, T., Qian, H., 2023. Metatranscriptome deciphers the effects of non-antibiotic antimicrobial agents on antibiotic resistance and virulence factors in freshwater microcosms. Aquat. Toxicol. 258, 106513.

Widenfalk, A., Bertilsson, S., Sundh, I., Goedkoop, W., 2008. Effects of pesticides on community composition and activity of sediment microbes – responses at various levels of microbial community organization. Environ. Pollut. 152, 576–584.

Woke, G., Aleleye-Wokoma, I., 2009. Effects of pesticide (Chlorpyrifos Ethyl) on the fingerlings of catfish (*Clarias gariepinus*). Glob. J. Pure Appl. Sci. 15, 3–4.

Wu, P., Zhang, Y., Chen, Z., Wang, Y., Zhu, F., Cao, B., Wu, Y., Li, N., 2019. The organophosphorus pesticides in soil was degradated by Rhodobacter sphaeroides after wastewater treatment. Biochem. Eng. J. 141, 247–251.

Xu, N., Zhao, Q., Zhang, Z., Zhang, Q., Wang, Y., Qin, G., Ke, M., Qiu, D., Peijnenburg, W. J.G.M., Lu, T., Qian, H., 2022. Phyllosphere microorganisms: sources, drivers, and their interactions with plant hosts. J. Agric. Food Chem. 70, 4860–4870.

Xu, N., Hu, H., Wang, Y., Zhang, Z., Zhang, Q., Ke, M., Lu, T., Penuelas, J., Qian, H., 2023. Geographic patterns of microbial traits of river basins in China. Sci. Total Environ. 871.

Xue, Y., Chen, H., Yang, J.R., Liu, M., Huang, B., Yang, J., 2018. Distinct patterns and processes of abundant and rare eukaryotic plankton communities following a reservoir cyanobacterial bloom. ISME J. 12, 2263–2277.
Xun, W., Li, W., Xiong, W., Ren, Y., Liu, Y., Miao, Y., Xu, Z., Zhang, N., Shen, Q., Zhang, R., 2019. Diversity-triggered deterministic bacterial assembly constrains community functions. Nat. Commun. 10, 3833.
Yu, Y., Zhang, Q., Zhang, Z., Xu, N., Li, Y., Jin, M., Feng, G., Qian, H., Lu, T., 2023. Assessment of residual chlorine in soil microbial community using metagenomics. Soil Ecol. Lett. 5, 66–78.
Yuan, M.M., Guo, X., Wu, Linwei, Zhang, Y., Xiao, N., Ning, D., Shi, Z., Zhou, X., Wu, Liyou, Yang, Y., Tiedje, J.M., Zhou, J., 2021. Climate warming enhances microbial network complexity and stability. Nat. Clim. Change 11, 343–348.
Zhang, Z., Fan, X., Peijnenburg, W.J.G.M., Zhang, M., Sun, L., Zhai, Y., Yu, Q., Wu, J., Lu, T., Qian, H., 2021. Alteration of dominant cyanobacteria in different bloom periods caused by abiotic factors and species interactions. J. Environ. Sci. 99, 1–9.
Zhang, Z., Wang, Y., Chen, B., Lei, C., Yu, Y., Xu, N., Zhang, Q., Wang, T., Gao, W., Lu, T., Gillings, M., Qian, H., 2022a. Xenobiotic pollution affects transcription of antibiotic resistance and virulence factors in aquatic microcosms. Environ. Pollut. 306, 119396.
Zhang, Z., Zhang, Q., Wang, T., Xu, N., Lu, T., Hong, W., Penuelas, J., Gillings, M., Wang, M., Gao, W., Qian, H., 2022b. Assessment of global health risk of antibiotic resistance genes. Nat. Commun. 13, 1553.
Zhou, Z., Zhang, Z., Feng, L., Zhang, J., Li, Y., Lu, T., Qian, H., 2020. Adverse effects of levofloxacin and oxytetracycline on aquatic microbial communities. Sci. Total Environ. 734, 139499.